

# Amorphous $\text{LiNiVO}_4$ thin-film anode for microbatteries grown by pulsed laser deposition

S.B. Tang, H. Xia, M.O. Lai, L. Lu\*

*Department of Mechanical Engineering, National University of Singapore, 117675 Singapore, Singapore*

Received 27 June 2005; accepted 24 October 2005

Available online 27 December 2005

## Abstract

Thin films of lithium nickel vanadates are deposited by pulsed-laser deposition from targets with different lithium contents. The as-deposited films are mainly amorphous and possess smooth and dense surfaces as revealed by X-ray diffraction and scanning-electron microscopy. The initial loss in capacity between the first discharge and charge decreases with increase in the lithium content in the films. The film grown from the target of  $\text{Li}_{1.2}\text{NiVO}_4$  gives the best performance with a retainable capacity as high as  $410 \mu\text{Ah per cm}^2 \mu\text{m}$ . There is almost no loss in capacity from the 11th up to the 50th cycle even though a fast decay occurs during the first several cycles. Cyclic voltammograms reveal cathodic peaks at 1.78 and 0.56 V and anodic peaks at 1.27 and 2.47 V, in line with the shapes of the discharge and charge curves.

© 2005 Elsevier B.V. All rights reserved.

*Keywords:* Pulsed-laser deposition; Lithium nickel vanadate; Anode; Capacity; Lithium thin-film microbatteries

## 1. Introduction

Rechargeable thin-film microbatteries are receiving more and more attention as low power sources for integrated microelectronics [1–3]. A thin-film microbattery is made up of a cathode, a solid electrolyte and an anode. In most studies, a metallic lithium film is employed as the anode. Due to its low melting point and strong reaction with air, however, lithium metal is not suitable for integration with micro-devices. There is therefore a need to replace the lithium anode with other stable thin-film materials. An amorphous silicon tin oxynitride anode (SiTON) with good thermal stability and recyclability has been developed [4].

Vanadates have been studied extensively for lithium-ion batteries [5–8].  $\text{LiNiVO}_4$  is particularly interesting among the various vanadate candidates since crystallized  $\text{LiNiVO}_4$  can be used both as a high-potential cathode [9] and as an anode [10,11]. In both crystallized and amorphous states, one  $\text{LiNiVO}_4$  ion can reversibly react with about seven lithium ions when it is discharged down to 0.02 V. This corresponds well with a specific capacity of  $920 \text{ mAh g}^{-1}$ , that is almost two and a half times the capacity of a graphite electrode. Bulk  $\text{LiNiVO}_4$  shows, however,

a low reversibility on the first cycle and a continuous capacity loss with further cycling. Recently, a  $\text{LiNiVO}_4$  thin-film anode has been deposited by radio frequency (rf) magnetron sputtering [12,13]. These amorphous thin films exhibit much better stability than the bulk materials [12], and their discharge capacity and stability are dependent on the composition and the conditions of the deposition process [13].

In the present study, the growth of an amorphous  $\text{LiNiVO}_4$  thin-film anode by pulsed-laser deposition (PLD) is reported for the first time, together with the results of electrochemical tests for its applicability in a rechargeable thin-film microbattery.

## 2. Experimental

$\text{LiNiVO}_4$  thin films were grown on both polished stainless-steel and silicon substrates by PLD from lithium nickel vanadate targets in a vacuum chamber. A 248 nm excimer laser beam with a power of 140 mJ per pulse and a repetition of 10 Hz was focused on to a target at an incidence angle of  $45^\circ$  (spot size of  $1 \text{ mm} \times 2 \text{ mm}$ ). The chamber was pumped to a base pressure of  $2 \times 10^{-5}$  Torr before oxygen was introduced. The oxygen pressure was kept at 8 mTorr and the temperature of the substrate was set at ambient temperature during deposition. The target was rotated and the substrate was placed on a holder held at a

\* Corresponding author. Tel.: +65 6874 2236; fax: +65 6779 1459.  
E-mail addresses: [luli@nus.edu.sg](mailto:luli@nus.edu.sg), [mpeluli@nus.edu.sg](mailto:mpeluli@nus.edu.sg) (L. Lu).

distance of 4 cm away from the target. Two targets with stoichiometric  $\text{LiNiVO}_4$  and Li-excess  $\text{Li}_{1.2}\text{NiVO}_4$  were used for deposition of the thin films. They were prepared by a similar solid-state reaction from mixtures of weighed  $\text{Li}_2\text{CO}_3$ ,  $\text{NiO}$  and  $\text{V}_2\text{O}_5$  powders at  $730^\circ\text{C}$  for 12 h in air [13]. The reacted mixtures were ground and pressed at  $100\text{ kg cm}^{-2}$  to form targets of 25 mm diameter. The final targets were formed by sintering at  $600^\circ\text{C}$  for 8 h.

Electrochemical tests were performed using a Solartron 1287 electrochemical interface. A home-made Swagelok cell was assembled using  $\text{LiNiVO}_4$  film of 10 mm diameter as the positive electrode and a Li metal foil as the negative electrode. The cell was placed in an argon-filled glove-box with both  $\text{H}_2\text{O}$  and  $\text{O}_2$  levels less than 0.1 ppm. The electrolyte was 1 M LiPF<sub>6</sub> in 1:1 ethylene carbonate (EC) and diethyl carbonate (DEC) solution (Merk). Charge and discharge cycling was performed between 3 and 0.02 V at a constant current density. Cyclic voltammetry (CV) was performed between 3 and 0.1 V at sweep rate of  $0.5\text{ mV s}^{-1}$ .

The surface morphology of the film was characterized by means of a Jeol 5600 scanning electron microscope (SEM). The thickness of the film was measured using a surface profiler (Tencor alpha-step 500). A Shimadzu XRD-6000 equipped with a Cu  $\text{K}\alpha$  source was used for crystalline phase analysis. The composition of the film was analyzed with a ICP-Optical Emission Spectroscopy (OES).  $\text{LiNiVO}_4$  films deposited on silicon substrates with a top layer of  $\text{SiO}_2$  ( $\sim 1.2\ \mu\text{m}$ ) were used for thickness measurement and composition analysis.

### 3. Results and discussion

The XRD  $\theta/2\theta$  spectra of the targets used for PLD and of the as-deposited thin films are shown in Fig. 1. In the stoichiometric  $\text{LiNiVO}_4$  target, very weak peaks of NiO are detected in addition to the main peaks of  $\text{LiNiVO}_4$  (Fig. 1(a)). In the excess lithium target of  $\text{Li}_{1.2}\text{NiVO}_4$ , both  $\text{Li}_3\text{VO}_4$  and NiO phases are observed (Fig. 1(b)), which indicates the coexistence of  $\text{LiNiVO}_4$ ,  $\text{Li}_3\text{VO}_4$  and NiO. By contrast, the thin film deposited at room temperature and 8 mTorr of oxygen pressure is mainly amorphous (Fig. 1(c)). The small peak at  $29.2^\circ$  in the thin film may be related to fine crystallites of  $\text{LiVO}_3$  that were not detected in the targets. Scanning electron micrographs (Fig. 2) show that the surfaces of the thin films are flat, uniform and dense without cracks and pinholes. A few particles are dispersed on the surfaces, which is a common feature of thin films deposited by PLD. The surface morphology of lithium nickel vanadate thin films grown by PLD appears to be much better than that of thin films deposited by rf magnetron sputtering except for some particles on the surfaces [12,13]. The composition of the films deposited from different targets are listed in Table 1. With increasing lithium content in the target, it is found that the relative content of lithium in the films significantly increases while the relative content of nickel increases only slightly. To achieve a Li:V ratio of above unity in the film grown by PLD, excess of lithium in the target is necessary to compensate for the loss of lithium during target preparation and deposition. The Ni:V ratio in the films deposited under the present conditions is not expected to be

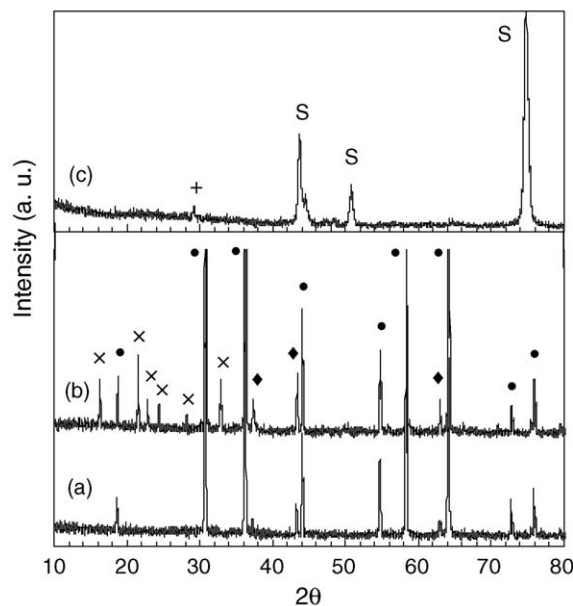


Fig. 1. XRD patterns of PLD targets and as-deposited thin films: (a)  $\text{LiNiVO}_4$  target; (b)  $\text{Li}_{1.2}\text{NiVO}_4$  target; (c) thin film grown from  $\text{Li}_{1.2}\text{NiVO}_4$  target at room temperature and 8 mTorr of oxygen (●,  $\text{LiNiVO}_4$ ; ◆, NiO; ×,  $\text{Li}_3\text{VO}_4$ ; +,  $\text{LiVO}_3$ ; S, stainless-steel substrate).

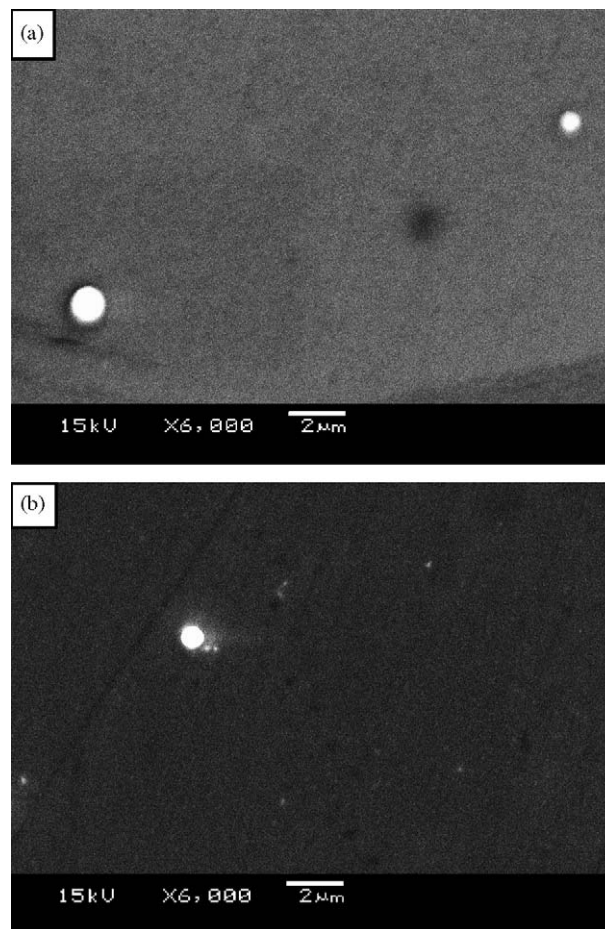


Fig. 2. Electron micrographs of surface of as-deposited thin films on stainless-steel substrates from targets of (a)  $\text{LiNiVO}_4$  and (b)  $\text{Li}_{1.2}\text{NiVO}_4$ .

Table 1  
Composition of thin films and initial irreversible capacity percentage of first cycle

Target	Film composition (atomic ratio Li:Ni:V)	Capacity of first discharge ( $\mu\text{Ah per cm}^2 \mu\text{m}$ )	Capacity of first charge ( $\mu\text{Ah per cm}^2 \mu\text{m}$ )	Irreversible capacity of first cycle (%)
$\text{LiNiVO}_4$	0.69:0.62:1	628.0	503.1	19.9
$\text{Li}_{1.2}\text{NiVO}_4$	0.96:0.65:1	570.8	511.5	10.4

much less than that in the stoichiometric ratio of the  $\text{LiNiVO}_4$  compound.

Discharge and charge curves on cycling the film grown from a target of  $\text{LiNiVO}_4$  are presented in Fig. 3. The initial section of the first discharge curve above 1.3 V is different from that of the following cycles. Moreover, it is also quite different from the first discharge curve of crystallized  $\text{LiNiVO}_4$  powder anode reported in reference [5]. The profiles of the discharge and charge curves from the second cycle onwards are, however, similar to each other. In particular, the curves for the 10th cycle are almost identical to those of the 50th cycle, which indicates that a relatively stable structure is formed during the first intercalation of lithium. The same trend is observed for films grown from a target of  $\text{Li}_{1.2}\text{NiVO}_4$ . Amorphous  $\text{LiNiVO}_4$  films grown by rf sputtering have been shown to exhibit similar curves [12]. It has been reported that an amorphous powder of  $\text{LiNiVO}_4 \cdot 2.6\text{H}_2\text{O}$  also displays a different discharge curve on the first cycle, with a reduction voltage ( $\sim 1.4$  V) that is lowest on the initial cycle. This may be due to the existence of moisture or internal re-ordering in the materials during the initial lithium intercalation. The charge and discharge curves of the present films deposited by PLD are typical of amorphous  $\text{LiNiVO}_4$  material, as confirmed further by XRD and SEM studies (Figs. 1 and 2).

Cyclic voltammetric (CV) curves for the thin-film electrode obtained from a target of  $\text{LiNiVO}_4$  at a scan rate of  $0.5 \text{ mV s}^{-1}$  after 50 cycles are given in Fig. 4. There is not only a broad cathodic peak at 1.78 V and a large sharp peak at around 0.56 V in the negative sweep from 3 to 0.1 V, but also two broad anodic peaks at 1.27 and 2.47 V. The peak positions in the CV scans are in line with the positions of the plateaus in the charge and discharge curves in Fig. 3. Moreover, the CV curves after 50 cycles

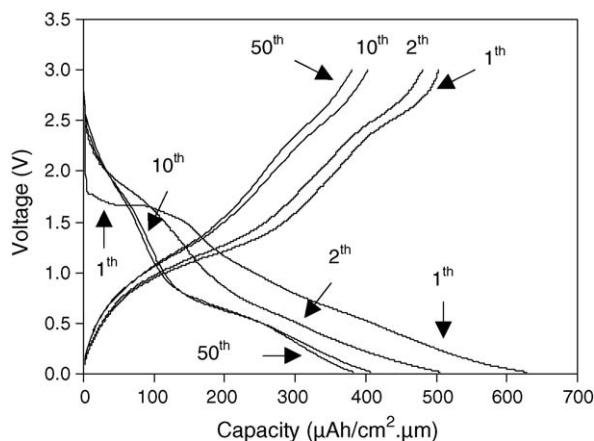


Fig. 3. Charge and discharge curves of thin-film electrode from target of  $\text{LiNiVO}_4$  at different number of cycles (current density =  $50 \mu\text{A cm}^{-2}$  for 1st and 2nd cycles and  $100 \mu\text{A cm}^{-2}$  for 10th and 50th cycles).

are quite repeatable during continuous scans, which suggests that the reduction and oxidation processes in the amorphous  $\text{LiNiVO}_4$  thin film are reversible. From ex situ X-ray absorption and electron energy loss measurements, Guyomard et al. [5] detected the reduction of vanadium cations from +5 down to +2.6 in a powder  $\text{LiNiVO}_4$  electrode with a lithium intercalation up to eight lithium per formula unit while the oxidation state of nickel was kept at almost +2. The cathodic peaks observed in the present study at 1.78 and 0.56 V during lithium intercalation may most likely correspond to different reduction states of vanadium.

The charge and discharge capacity as a function of cycle number for thin-film electrodes grown from targets of  $\text{LiNiVO}_4$  and  $\text{Li}_{1.2}\text{NiVO}_4$  are shown in Fig. 5. During the first reduction, a discharge as high as  $628 \mu\text{Ah per cm}^2 \mu\text{m}$  is delivered by the thin-film electrode obtained from the  $\text{LiNiVO}_4$  target (Fig. 5(a)). It can be deduced that partially-inserted lithium cannot be removed during the first charge. The charge capacity on the first cycle is about  $503 \mu\text{Ah per cm}^2 \mu\text{m}$ , which corresponds to 19.9% of the irreversible capacity loss between the first discharge and charge (Table 1). The capacity decays rapidly during the first few cycles. From the 11th cycle onwards, the capacity becomes relatively stable; there is a decay of only 0.12% per cycle. The film deposited from a lithium-excess target of  $\text{Li}_{1.2}\text{NiVO}_4$  experiences only 10.4% loss of initial capacity during the first cycle although the capacity of the first discharge decreases to  $570.8 \mu\text{Ah per cm}^2 \mu\text{m}$  (Fig. 5(b)). Moreover, it should be noted that this film becomes very stable after 10

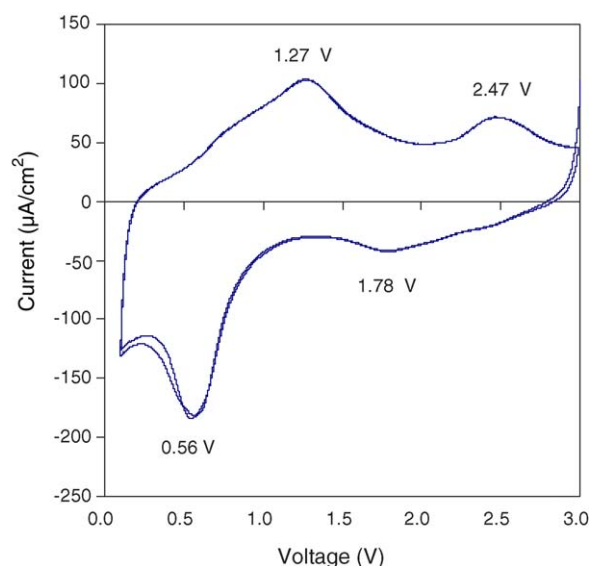


Fig. 4. Cyclic voltammograms for thin-film electrode from target of  $\text{LiNiVO}_4$  at scan rate of  $0.5 \text{ mV s}^{-1}$  after film discharged and charged for 50 cycles.

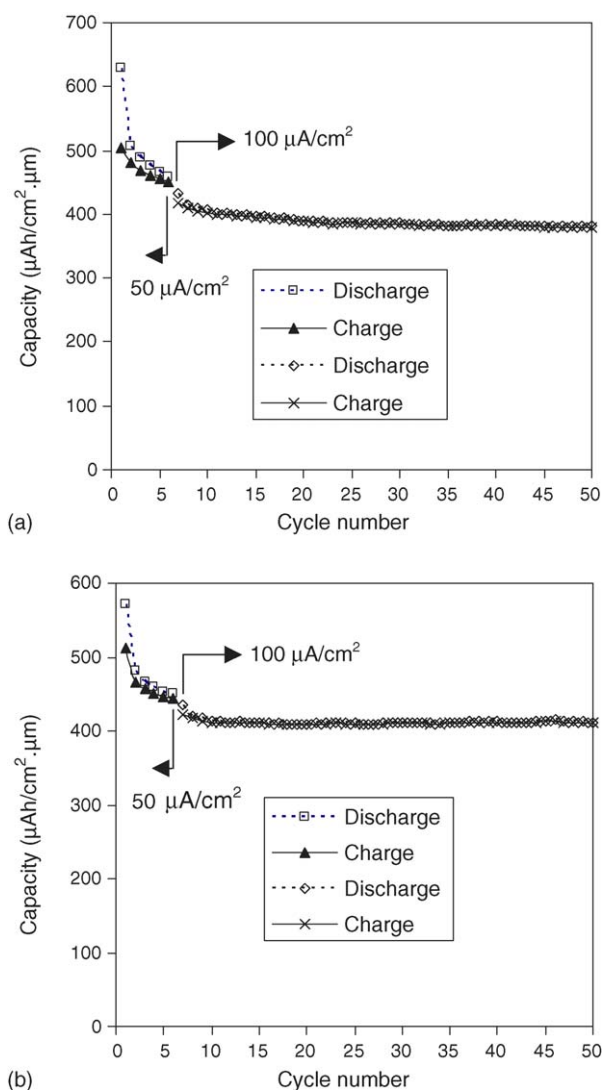


Fig. 5. Discharge and charge capacity vs. cycle number for thin-film electrodes from target of (a)  $\text{LiNiVO}_4$  and (b)  $\text{Li}_{1.2}\text{NiVO}_4$  (current density =  $50 \mu\text{A cm}^{-2}$  for first six cycles and  $100 \mu\text{A cm}^{-2}$  for cycles 7–50).

cycles. There is almost no observable decay in capacity while the coulombic efficiency is nearly 100% from the 11th to the 50th cycle. A reversible capacity of  $410 \mu\text{Ah per cm}^2 \mu\text{m}$ , almost six times the feasible capacity of a  $\text{LiCoO}_2$  thin-film cathode ( $69 \mu\text{Ah per cm}^2 \mu\text{m}$  for  $\text{Li}_{0.5}\text{CoO}_2$ ) [14], is retainable. This value corresponds to a capacity of  $1025 \text{mAh g}^{-1}$  if bulk density of  $\text{LiNiVO}_4$  ( $\sim 4 \text{g cm}^{-3}$ ) is assumed for the film, which is higher than the capacity obtained from  $\text{LiNiVO}_4$  power materials ( $920 \text{mAh g}^{-1}$ ) and more than 2.5 times the capacity of a graphite electrode [11]. The specific capacity of the present film grown from  $\text{Li}_{1.2}\text{NiVO}_4$  target is close to that of a  $\text{Li}_{1.1}\text{NiVO}_4$  film ( $400 \mu\text{Ah per cm}^2 \mu\text{m}$ ) reported by Reddy et al. [13], but lower than that of a  $\text{Li}_{1.8}\text{Ni}_{0.8}\text{VO}_{3.8}$  film ( $871 \mu\text{Ah per cm}^2 \mu\text{m}$ ) published by Lee et al. [12], both of which were grown by rf magnetron sputtering. The large difference in capacity may be due to the difference in composition of the films or errors in the measurement of their thickness given the small thickness ( $\sim 200 \text{nm}$ ) and the roughness of the surface of the films.

It is noted that the irreversible capacity loss between the first charge and discharge decreases with increasing lithium content in the films, as shown in Table 1. The initial capacity loss of about 10.4% for the thin film deposited from a target of  $\text{Li}_{1.2}\text{NiVO}_4$  where the Li:V ratio is 0.96, which is close to the stoichiometric ratio of  $\text{LiNiVO}_4$ , is much less than the 30% loss from amorphous  $\text{LiNiVO}_4 \cdot 2.6\text{H}_2\text{O}$  powder. The cycling stability of the thin film grown from a target of  $\text{Li}_{1.2}\text{NiVO}_4$  is also much better than that of a powder electrode [11] and that of a film grown from a target of  $\text{LiNiVO}_4$ . It is not certain whether the Ni:V ratio plays an important role in the capacity and the cycling stability of the thin films as suggested by Reddy et al. [13] since the difference in the Ni:V ratios in the present two films is not too large. It seems reasonable that the film with more lithium content retains less lithium after the first discharge. This indicates that the capacity loss during the first cycle and its stability is dependent on the composition of the films. Further experimentation is required to optimize the film composition so as to improve its electrochemical properties.

#### 4. Conclusions

Uniform and dense amorphous thin films of lithium nickel vanadates without cracks and pinholes have been successfully grown by pulsed laser deposition. The electrochemical properties of these films, especially capacity loss between the first discharge and charge, depends on the composition of the films. The film grown from a lithium excess target of  $\text{Li}_{1.2}\text{NiVO}_4$  shows only 10.4% of initial capacity loss during the first cycle and  $410 \mu\text{Ah per cm}^2 \mu\text{m}$  of capacity is maintained between cycles 10 and 50. This capacity is more than 2.5 times greater than that of a graphite anode. These results suggest that the thin films offer promising application in microbatteries.

#### Acknowledgement

This work has been supported by the National University of Singapore under research grants R265-000-133-112 and R265-000-162-112.

#### References

- [1] J.B. Bates, N.J. Dudney, B. Neudecker, A. Ueda, C.D. Evans, *Solid State Ionics* 135 (2000) 33.
- [2] B.J. Neudecker, N.J. Dudney, J.B. Bates, *J. Electrochem. Soc.* 147 (2000) 517.
- [3] N. Kuwata, J. Kawamura, K. Toribami, T. Hattori, N. Sata, *Electrochem. Commun.* 6 (2004) 417.
- [4] B.J. Neudecker, R.A. Zuhr, J.B. Bates, *J. Power Sources* 81 (1999) 27.
- [5] D. Guyomard, C. Sigala, A. Le Gal La Salle, Y. Piffard, *J. Power Sources* 68 (1997) 692.
- [6] C. Julien, E. Haro-Poniatowska, M.A. Camacho-Lopez, L. Escobar-Alarcon, J. Jimenez-Jarquín, *Mater. Sci. Eng. B65* (1999) 170.
- [7] E. Baba Ali, J.C. Bernede, D. Guyomard, *Thin Solid Films* 402 (2002) 215.
- [8] C.M. Julien, *Mater. Sci. Eng. R40* (2003) 47.
- [9] M. Arrabito, S. Bodoardo, N. Penazzi, S. Panero, P. Reale, B. Scrosati, Y. Wang, X. Guo, S.G. Greenbaum, *J. Power Sources* 97–98 (2001) 478.
- [10] C. Rossignol, G. Ouvrard, E. Baudrin, *J. Electrochem. Soc.* 168 (2001) A869.



- [11] F. Orsini, E. Baudrin, S. Denis, L. Dupont, M. Touboul, D. Guyomard, Y. Piffard, J.-M. Tarascon, *Solid State Ionics* 107 (1998) 123.
- [12] S.-J. Lee, H.-Y. Lee, T.-S. Ha, H.-K. Baik, S.-M. Lee, *Electrochem. Solid State Lett.* 5 (2002) A138.
- [13] M.V. Reddy, C. Wannek, B. Pecquenard, P. Vinatier, A. Levasseur, J. Power Sources 119–121 (2003) 101.
- [14] K.W. Kim, S.I. Woo, K.-H. Choi, K.-S. Han, Y.-J. Park, *Solid State Ionics* 159 (2003) 25.